Progress In Electromagnetics Research C, Vol. 71, 133–140, 2017

Triple-Band Composite Right/Left Handed Bandpass Filter Using a New Circular Inter-Digital Capacitor for Wireless Applications

Ashish Kumar, Dilip Kumar Choudhary, and Raghvendra Kumar Chaudhary*

Abstract—In this paper, a compact triple-band bandpass filter based on composite right/left handed (CRLH) approach has been proposed. The zeroth order resonance (ZOR) frequency of the designed filter can be controlled effectively by varying the series parameters. A new circular interdigital capacitor is integrated to provide series capacitance. The number of passbands depends on number of rings of circular interdigital capacitor (C-IDC). In order to validate metamaterial behavior, a dispersion diagram has been plotted for the designed filter. The proposed filter offers measured 3 dB fractional bandwidth of 71% at 1.7 GHz, 24% at 2.9 GHz and 12% at 4.1 GHz as center frequencies. The designed filter will be suitable for different wireless applications such as global navigation satellite systems (1.559–1.610 GHz), GSM1800, indoor femtocells (2.5–2.7 GHz), air traffic surveillance (2.7–2.9 GHz) and fixed satellite services (3.8–4.2 GHz). The size of the proposed filter is $0.13\lambda_0 \times 0.11\lambda_0$, where λ_0 is the free space wavelength at ZOR frequency of 1.7 GHz.

1. INTRODUCTION

Increasing demands for wireless services and rapid growth in wireless communication technology creates a need for miniaturization and multiband services, and this makes multiband filters a very interesting solution. Hence, multi-band bandpass filters with low insertion loss, compact size and ease of integration are of great interest. Numerous techniques have been introduced to design multiband bandpass filters [1–7]. The number of passbands can be increased by cascading coupled resonators in a single filter structure [1]. Three pairs of coupled resonators are arranged in a multi-layered substrate to achieve size reduction and offers a cross-coupling effect simultaneously [2]. The sharpness of the passband depends upon the arrangement of the cross-coupling configuration of the stepped-impedance resonators [3–5]. The bandwidth of a triple-band bandpass filter can be controlled by using short stub loaded stub impedance resonator, and transmission zero can be increased by embedded stepped impedance resonators [6, 7]. Interdigital capacitor techniques are used to reduce the size of the resonator [8–10]. In the last decade, metamaterial (MTM) evolves as an alternative for filter applications. Using MTM, filters can be made compact as it follows the effective-homogeneity condition [11] and various other features, which makes it revolutionary in wireless communication. MTM is an artificially constructed periodic electromagnetic structure with both negative permittivity and permeability. Left-handed (LH) material was first investigated theoretically in 1968 by Russian physicist Viktor Veselago [12]. The transmission line (TL) approach of LH materials was presented by cascading the series capacitors and shunt inductances to support a medium with negative refractive index [13, 14]. LH material shows backward-wave propagation by forming a left-handed triplet among the propagated magnetic field, electric field and wave number vector. Implementation of the LH TL produces parasitic series inductance and shunt capacitance which form composite right/left-handed (CRLH) TL [11].

Received 29 December 2016, Accepted 3 February 2017, Scheduled 13 February 2017

* Corresponding author: Raghvendra Kumar Chaudhary (raghvendra.chaudhary@gmail.com).

The authors are with the Department of Electronics Engineering, Indian Institute of Technology (Indian School of Mines), Dhanbad-826004, India.

In this paper, a new CRLH triple-band bandpass filter is proposed using a new circular interdigital capacitor (C-IDC) and circular stub, where the stub is shorted to the ground plane through a via. The scattering parameters, group delay and dispersion diagram of the designed filter and its equivalent electric circuit are presented. The triple-band bandpass filter is designed for frequencies ranging from 0.9 to 1.9 GHz, 2.43 to 3.1 GHz and 3.8 to 4.3 GHz, with an average insertion loss less than 1 dB in the passbands. The electrical size of designed filter is $0.13\lambda_0 \times 0.11\lambda_0$ at the zeroth order resonance (ZOR) frequency 1.7 GHz, where λ_0 is free space wavelength.

2. FILTER DESIGN THEORY

The layout of the proposed triple-band bandpass filter and its lossy equivalent electrical circuit is shown in Figure 1 and Figure 2. The proposed structure uses vias and creates a short ended structure.

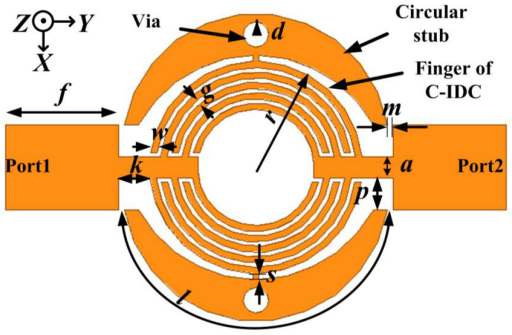

Figure 1. Layout of proposed filter [All dimensions are in mm: $r = 7.4$, $w = 0.3$, $g = 0.2$, $l = 21.2$, $d = 0.6$, $f = 5.4$, $s = 0.3$, $a = 1$, $p = 1.55$, $k = 1.6$, $m = 0.2$].

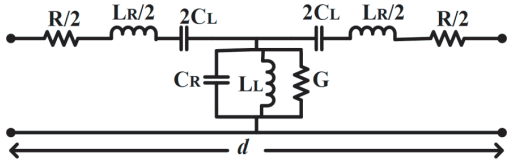

Figure 2. Lossy equivalent circuit diagram of proposed filter.

This design shows series capacitance C_L due to the gap between fingers of the circular IDC and shunt inductance L_L due to circular stubs which are shorted to the ground plane through via. Right-handed (RH) inductance L_R represents combination of series inductances resulting from feed line and parasitic inductances. The parasitic inductance is generated because of magnetic flux induced in circular IDC. The parasitic capacitance C_R is generated due to the voltage gradient existing between fingers of circular IDC and ground plane. Series resistance R and shunt conductance G are the loss factors.

The combination of a circular stub and shorted via line provides effective inductance to support backward wave propagation over passbands. The CRLH TL dispersion relation can be explained theoretically by applying the Bloch-Floquet theorem on the ABCD matrix of the proposed equivalent circuit [15] as:

$$\beta(\omega) = \frac{1}{d}\cos^{-1}\left(1 + Z\left(\omega\right)Y\left(\omega\right)\right) \tag{1}$$

$$\beta(\omega) = \frac{1}{d}\cos^{-1}\left(1 - \left(\frac{\omega^2}{\omega_R^2} + \omega_L^2\left(\frac{1}{\omega^2} - \frac{1}{\omega_{Sh}^2} - \frac{1}{\omega_{Se}^2}\right)\right)\right) \tag{2}$$

where, $Z\left(\omega\right) = \frac{1}{j\omega C_L} + j\omega L_R$, $Y\left(\omega\right) = \frac{1}{j\omega L_L} + j\omega C_R$, $\omega_L = \frac{1}{\sqrt{L_L C_L}}, \omega_R = \frac{1}{\sqrt{L_R C_R}}$, shunt resonance frequency $(\omega_{Sh}) = \frac{1}{\sqrt{L_L C_R}}$, series resonance frequency $(\omega_{Se}) = \frac{1}{\sqrt{L_R C_L}}$, d is the physical length of unit cell, and β is the propagation constant. The ZOR frequency is decided by series parameter as structure is short ended. The cutoff frequencies of the passbands can be evaluated for $\beta\left(\omega\right)d = 0$ or π. Putting the value of $\beta\left(\omega\right)d = 0$ in Eq. (2),

$$-\frac{\omega^2}{\omega_R^2} - \frac{\omega_L^2}{\omega^2} + \frac{\omega_L^2}{\omega_{Sh}^2} + \frac{\omega_L^2}{\omega_{Se}^2} = 0 \tag{3}$$

$$\omega^4 M - \omega^2 N + K = 0 \tag{4}$$

Similarly, for $\beta(\omega)\, d = \pi$ Eq. (2) becomes

$$\omega^4 - \omega^2 P + Q = 0 \tag{5}$$

where, $\omega_{sh}^2\omega_{se}^2 = M$, $\omega_R^2\omega_L^2\omega_{se}^2 + \omega_R^2\omega_L^2\omega_{sh}^2 = N$ and $\omega_R^2\omega_L^2\omega_{se}^2\omega_{sh}^2 = K$, $\omega_R^2 x + 2\omega_R^2 = P$, $\omega_R^2\omega_L^2 = Q$ and $\frac{\omega_L^2}{\omega_{sh}^2} + \frac{\omega_L^2}{\omega_{se}^2} = x$. The dispersion relation equations as shown in Eq. (4) and Eq. (5) become fourth order, hence such types of filter can carry a maximum of four passbands. Thus, the cutoff frequency (ω_{Co}) of proposed filter can be calculated from Eq. (4) and Eq. (5) as

$$\omega_{co}^2 = \frac{N \pm \sqrt{N^2 - 4KM}}{2M}, \frac{P \pm \sqrt{P^2 - 4Q}}{2} \tag{6}$$

The proposed filter has eight cutoff frequencies (as it has a maximum of four passbands), which can be calculated using Eq. (6). The center frequencies ω_c of the above passbands are obtained at $\beta(\omega)d = \pi/2$

$$\frac{\omega_c^4}{\omega_L^2\omega_R^2} - \omega_c^2\left(\frac{1}{\omega_L^2} + \frac{1}{\omega_{Sh}^2} + \frac{1}{\omega_{Se}^2}\right) + 1 = 0 \tag{7}$$

$$\omega_c^4\omega_l - \omega_c^2\omega_k + 1 = 0 \tag{8}$$

$$\omega_c^2 = \frac{\omega_k \pm \sqrt{\omega_k^2 - 4\omega_l}}{2\omega_l} \tag{9}$$

where, $\omega_k = \frac{1}{\omega_L^2} + \frac{1}{\omega_{sh}^2} + \frac{1}{\omega_{se}^2}$, and $\omega_l = \frac{1}{\omega_L^2\omega_R^2}$. Using Eq. (9), the centre frequency of the proposed design can be determined. To confirm the backward wave propagation, a dispersion diagram can be used, where a negative slope shows anti-parallel phase and group velocity. The dispersion relation of the proposed triple-band bandpass filter is obtained by plotting Eq. (10) as shown below [16].

$$\beta = \frac{1}{d}\left(\frac{1 - S_{11}S_{22} + S_{12}S_{21}}{2 \times S_{21}}\right) \tag{10}$$

where S_{11}, S_{22} are reflection coefficients, and S_{21}, S_{12} are transmission coefficients. The transition time of a signal across a network is defined by group delay (t_{gd}). This can be calculated using Eq. (11) as the negative slope of insertion phase response with respect to frequency [17].

$$t_{gd} = \frac{-1}{360^\circ} \times \frac{\partial\theta}{\partial f} \tag{11}$$

where θ is the insertion phase in degrees, and f is the frequency. Selecting a lower aperture (frequency step) in the vector network analyzer during measurement results in high group delay but favors high resolution.

3. FABRICATION AND RESULT

The proposed triple-band bandpass filter is designed and analyzed using high frequency structural simulator ANSYS HFSS 14.0 3D simulation software. The proposed filter is fabricated on an FR4 substrate (with a thickness of 1.6 mm, dielectric constant $\varepsilon_r = 4.4$ and loss tangent of 0.02) as shown in Figure 3. The scattering parameters, group delay and dispersion relations of the fabricated filter are measured using an Agilent N5221A Vector Network Analyzer.

Simulated and measured scattering parameters of the prototype are compared in Figure 4. The measured result shows a maximum insertion loss of 0.5 dB, 0.8 dB and 1.9 dB at the first, second and third passbands, respectively. The third band insertion loss increases compared to the simulated result due to imperfection in the shorting via. There is a glitch and slight shift in group delay from the measured result compared to simulation, as shown in Figure 5. The shift is about 100 MHz, but results confirm that the group delay is reasonably flat over the pass-bands. The proposed design shows an average group delay of less than 1 ns in the pass-bands. The measured and simulated dispersion diagrams of designed filter are shown in Figure 6.

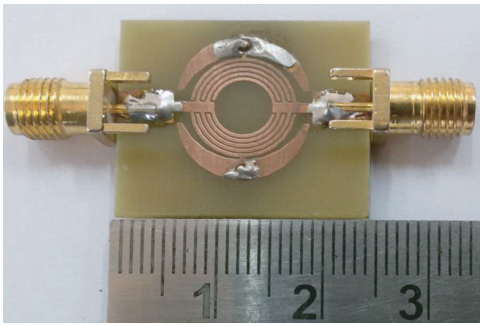

Figure 3. Fabricated prototype of designed triple band bandpass filter.

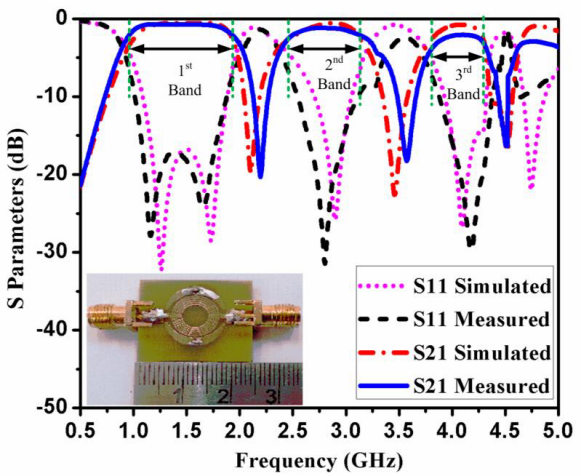

Figure 4. Simulated and measured scattering parameter of proposed bandpass filter.

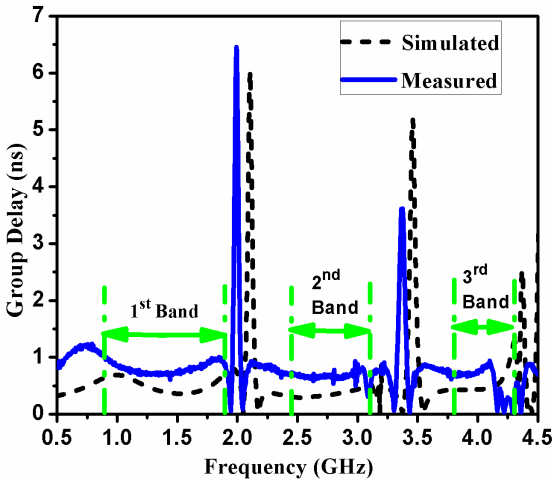

Figure 5. Simulated and measured group delay of proposed band bandpass filter.

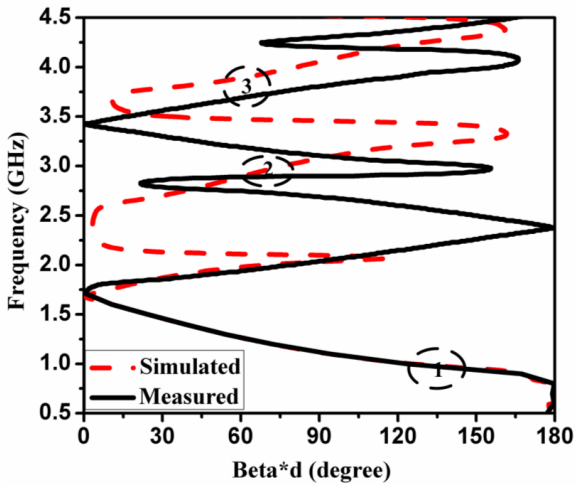

Figure 6. Simulated and measured dispersion diagram for proposed filter.

Considering the simulated values of frequencies in Figure 6, it shows an extension of the first band with negative slope from 0.9 to 1.7 GHz which confirms it as a LH band. The second band extends from 2.43 to 3.1 GHz with positive slope which validates it to be a RH band. The third band is a RH band ranging from 3.8 to 4.3 GHz. The measured dispersion diagram shows a little deviation from the simulated result due to imperfection in fabrication.

4. ANALYSIS AND JUSTIFICATION OF RESULTS FOR PROPOSED FILTER

The proposed filter structure is implemented using circular IDC, circular stub and shorted via line. Here, a via plays an important role in realizing the MTM property for the proposed filter. The reactance value of the via is related to S-parameters using standard formulas [18] as

$$L_V = \frac{Z_0}{\omega} img\left(\frac{1+S_{11}}{1-S_{11}}\right) \tag{12}$$

$$C_V = \frac{1}{\omega Z_0} img\left(\frac{1-S_{11}}{1+S_{11}}\right) \tag{13}$$

where, Z_0 is the characteristic impedance, and S_{11} is the input reflection coefficient. L_v and C_v represent via inductance and parasitic capacitance due to via, where C_v is due to transition of charge density from the circular stub to the via. The electromagnetic (EM) energy transmitted from top to bottom is controlled by the radius of the via. The insertion loss in the proposed design increases in between passbands by increasing the radius of the via. This is due to excessive reflection of EM energy with increase of via radius, which results in poor S_{21} [19]. Via inductance (L_v) and parasitic via capacitance (C_v) are obtained by using Eq. (12) and Eq. (13) as shown in Figure 7. The value of C_v is negligible (required), and L_v is small in passbands. Figure 7 confirms the independence of ZOR from C_v and L_v which are the shunt parameters for the structure.

The variations for frequency response with respect to via holes size are shown in Figure 8. While increasing the radius of via holes the 2nd and 3rd passbands shift towards higher frequency. The proposed filter follows short-ended condition, so less influence on passband due to shunt inductance (due to via). It mainly depends on series parameters due to short-ended boundary condition.

The bandwidth of each passband can be controlled by varying the gap of C-IDC (g), which is shown in Figure 9. By increasing the gap (g), the bandwidths of 1st and 2nd passbands increase, and 3rd passband bandwidth decreases.

Variation in the ZOR frequency with change in the gap of C-IDC (g) shown in the dispersion diagram is shown in Figure 10. As the gap between the fingers of C-IDC increases, C_L decreases, which shifts ZOR frequency to a higher value. This can be evaluated as, for short ended, ZOR input impedance

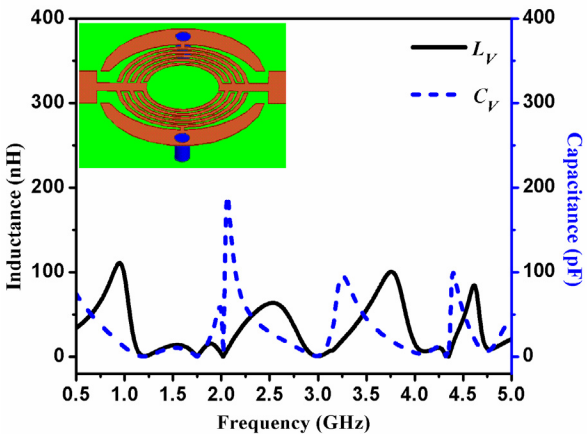

Figure 7. Variation of L_V and C_V of designed filter with respect to frequency.

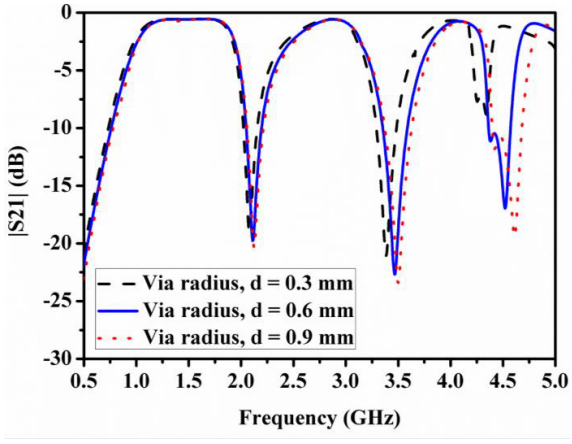

Figure 8. Variation of radius of via holes with respect to frequency.

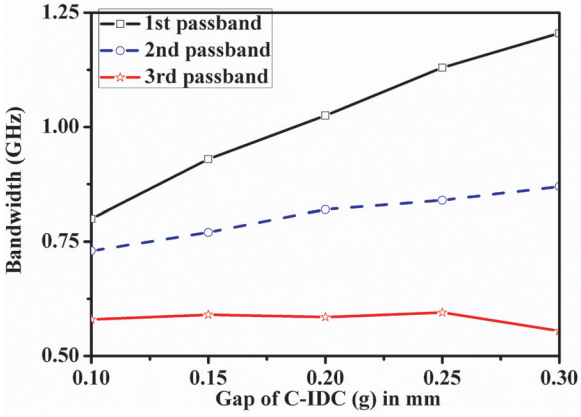

Figure 9. Variation in bandwidth by changing the gap of C-IDC.

$\left(Z_{in}^{Short}\right)$ seen from one end to another end of resonator which is given by,

$$Z_{in}^{Short} = -jZ_0 \tan(\beta l)^{\beta \to 0} = -jZ_0\beta l$$
$$= -j\sqrt{\frac{Z(\omega)}{Y(\omega)}}\left(j\sqrt{Z(\omega)Y(\omega)}\right) l = Z(\omega)l = Z(\omega)N \quad (14)$$

where N is the number of unit cells, and l is the length of designed filter ($l = N \cdot d$). Eq. (14) shows that the short-ended ZOR frequency only depends on the resonance of the series parameters. Thus, the resonant frequency (ω_{rs}) of the short-ended TL depends on the series parameters only.

$$\omega_{rs} = \frac{1}{\sqrt{C_L L_R}} \quad (15)$$

It is observed from the simulation results that the number of passbands in a specified band is dependent on number of rings (N_{Ring}) of the C-IDC. Figure 11 shows that as N_{Ring} increases, the number of passbands of the filter increases in the specified band because of the increase in values of the series parameters.

Variation in group delay due to different widths of fingers of the C-IDC is shown in Figure 10. It shows that by increasing the finger width of the circular IDC, group delay increases between passbands.

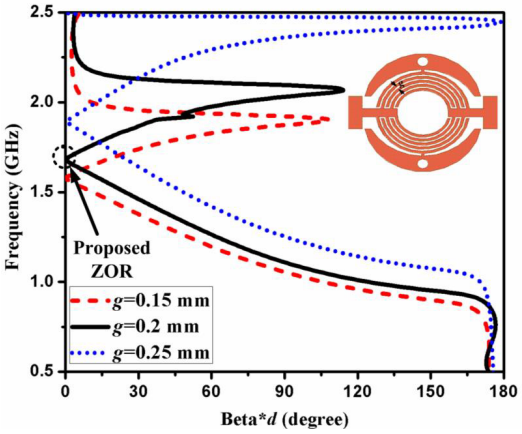

Figure 10. Variation in ZOR frequency with change in gap of C-IDC (g).

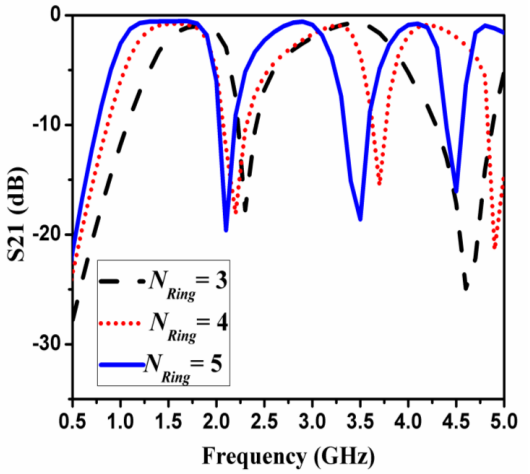

Figure 11. Simulated insertion loss of proposed filter with varying N.

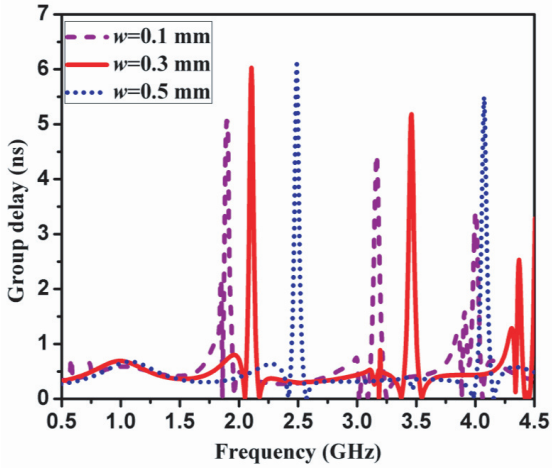

Figure 12. Variation in group delay for different width of finger of C-IDC (w).

The higher value of group delay has been caused by attenuation of S_{21} in between pass bands. It has also been observed that there is a small variation in group delay within the passband as shown in Figure 12, which is required for signal transmission with minimum distortion.

To justify the proposed structure, a comparison of performance with earlier published triple-band filters is shown in Table 1, which shows that the proposed filter has advantages of low insertion loss, wide 3 dB fractional bandwidth (FBW) with compact size.

Table 1. Comparison with earlier published triple band bandpass filter.

Ref.	1st/2nd/3rd Passbands (GHz)	Insertion loss (dB)	Insertion loss (dB)	FBW (%)	Dimensions ($\lambda_0 \times \lambda_0$)
[1]	2.3/3.7/5.3	2.5/1.9/2.9	> 18	3.9/7/5.2	0.44×0.39
[3]	1.57/2.45/3.5	0.77/1.51/1.8	> 20	12.5/8/6	0.18×0.1
[4]	1.575/2.4/3.5	1.6/1.5/2.3	9/18.9/13.5	5.2/3.8/4.6	0.72×0.82
[5]	2.45/3.5/5.25	0.9/0.7/2.1	> 13	12.3/6.2/3.3	0.26×0.32
[17]	2.45/3.5/5.25	2/2.4/1.7	18/16/13	2.5/1.7/5	0.19×0.18
This work	1.7/2.9/4.1	0.5/0.8/1.9	25.5/32.7/31.5	71/24/12	0.13×0.11

5. CONCLUSION

A compact triple-band bandpass filter based on CRLH-TL using a circular IDC is designed. In this paper, the proposed filter has three passbands from 0.9-1.9 GHz, 2.43–3.1 GHz and 3.8–4.3 GHz. The measured insertion losses are 0.5 dB, 0.8 dB and 1.9 dB in the first, second and third frequency bands, respectively. An attenuation of more than 17 dB is obtained between the passbands. The return losses are 25.5 dB, 32.7 dB and 31.5 dB at center frequencies of 1.7 GHz, 2.9 GHz and 4.1 GHz, respectively. The experimental results are close to simulated ones, which validates the proposed triple-band bandpass filter. The proposed filter has an electrical size of $0.13\lambda_0 \times 0.11\lambda_0$ at the ZOR frequency. The possible application of the triple-band bandpass filter may be global navigation satellite systems (1.559–1.610 GHz), GSM1800, indoor femtocells (2.5–2.7 GHz), air traffic surveillance (2.7–2.9 GHz) and fixed satellite services (3.8–4.2 GHz).

REFERENCES

1. Chen, C., T. Huang, and R. Wu, "Design of dual and triple-passband filters using alternately cascaded multiband resonators," *IEEE Transactions on Microwave Theory and Techniques*, Vol. 54, 3550–3558, 2006.
2. Weng, M., H. Wu, K. Shu, J. Chen, R. Yang, and Y. Su, "A novel triple-band bandpass filter using multilayer-based substrates for WiMAX," *37th European Microwave Conference, European*, 325–328, 2007.
3. Hsu, C. G., C. Lee, and Y. Hsieh, "Tri-band bandpass filter with sharp passband skirts designed using tri-section SIRs," *IEEE Microwave and Wireless Components Letters*, Vol. 18, 19–21, 2008.
4. Chen, W., M. Weng, and S. Chang, "A new tri-band bandpass filter based on stub-loaded step-impedance resonator," *IEEE Microwave and Wireless Components Letters*, Vol. 22, 179–181, 2012.
5. Lai, X., C. H. Liang, H. Di, and B. Wu, "Design of tri-band filter based on stub loaded resonator and DGS resonator," *IEEE Microwave and Wireless Components Letters*, Vol. 20, 265–267, 2010.
6. Xu, K., Y. Zhang, D. Li, Y. Fan, J. L. Wei, W. T. Joines, and Q. H. Liu, "Novel design of a compact triple-band bandpass filter using short stub-loaded sirs and embedded sirs structure," *Progress In Electromagnetics Research*, Vol. 142, 309–320, 2013.

7. Chiou, Y. C. and J. T. Kuo, "Planar multiband bandpass filter with multimode stepped-impedance resonators," *Progress In Electromagnetics Research*, Vol. 114, 129–144, 2011.
8. Shen, W., W. Yin, X. Sun, and J. Mao, "A new wide stopband microstrip bandpass filter with miniaturized interdigital capacitor resonator," *Electrical Design of Advanced Packaging & Systems Symposium*, 1–5, Hong Kong, 2009.
9. Sam, S., H. Kang, and S. Lim, "Frequency reconfigurable and miniaturized substrate integrated waveguide interdigital Capacitor (SIW-IDC) antenna," *IEEE Transactions on Antennas and Propagation*, Vol. 62, 1039–1045, 2014.
10. Fouad, M. A. and M. A. Abdalla, "New π-T generalised metamaterial negative refractive index transmission line for a compact coplanar waveguide triple band pass filter applications," *IET Microwave and Antennas Propagation*, Vol. 8, 1097–1104, 2014.
11. Caloz, C. and T. Itoh, *Electromagnetic Metamaterials: Transmission Line Theory and Microwave Applications*, John Wiley & Sons, Inc., 2006.
12. Veselago, V., "The electrodynamics of substances with simultaneously negative values of ε and μ," *Soviet Physics Uspheki*, Vol. 10, 509–514, 1968.
13. Caloz, C. and T. Itoh, "Application of the transmission line theory of left-handed (LH) materials to the realization of a microstrip LH line," *IEEE Antennas and Propagation Society International Symposium*, Vol. 2, 412–415, 2002.
14. Iyer, A. K. and G. V. Eleftheriades, "Negative refractive index metamaterials supporting 2-D waves," *Int. Microwave Symp.*, Vol. 2, 1067–1070, June 2002.
15. Sanada, A., K. Murakami, S. Aso, H. Kubo, and K. Awai, "A via-free microstrip left-handed transmission line," *Microwave Symposium Digest*, Vol. 1, 301–304, 2004.
16. Choudhary, D. K. and R. K. Chaudhary, "Vialess wideband bandpass filter using CRLH transmission line with semi-circular stub," *2nd International Conference on Microwave and Photonics (ICMAP)*, 1–2, 2015.
17. "RF design and seminar and measurement seminar," 187, Hewlett Packard, Appendix.
18. Low, H., M. K. Iyer, B. Ooi, and M. Bong, "Via design optimisation for high speed device packaging," *2nd International Conference on Electronics Packaging Technology*, 112–118, Singapore, 1998.
19. Chen, F. C. and Q. X. Chu, "Design of compact tri-band bandpass filters using assembled resonators," *IEEE Transactions on Microwave Theory and Techniques*, Vol. 57, 165–171, 2009.